Accepted Manuscript

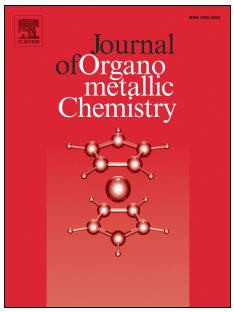

Periodical trends in $[Co_6E(CO)_{16}]$- clusters: Structural, synthetic and energy changes produced by substitution of P with As

Roberto Della Pergola, Annalisa Sironi, Valentina Colombo, Luigi Garlaschelli, Stefano Racioppi, Angelo Sironi, Piero Macchi

PII: S0022-328X(17)30345-5

DOI: 10.1016/j.jorganchem.2017.05.041

Reference: JOM 19967

To appear in: *Journal of Organometallic Chemistry*

Received Date: 27 January 2017

Accepted Date: 18 May 2017

Please cite this article as: R. Della Pergola, A. Sironi, V. Colombo, L. Garlaschelli, S. Racioppi, A. Sironi, P. Macchi, Periodical trends in $[Co_6E(CO)_{16}]$- clusters: Structural, synthetic and energy changes produced by substitution of P with As, *Journal of Organometallic Chemistry* (2017), doi: 10.1016/j.jorganchem.2017.05.041.

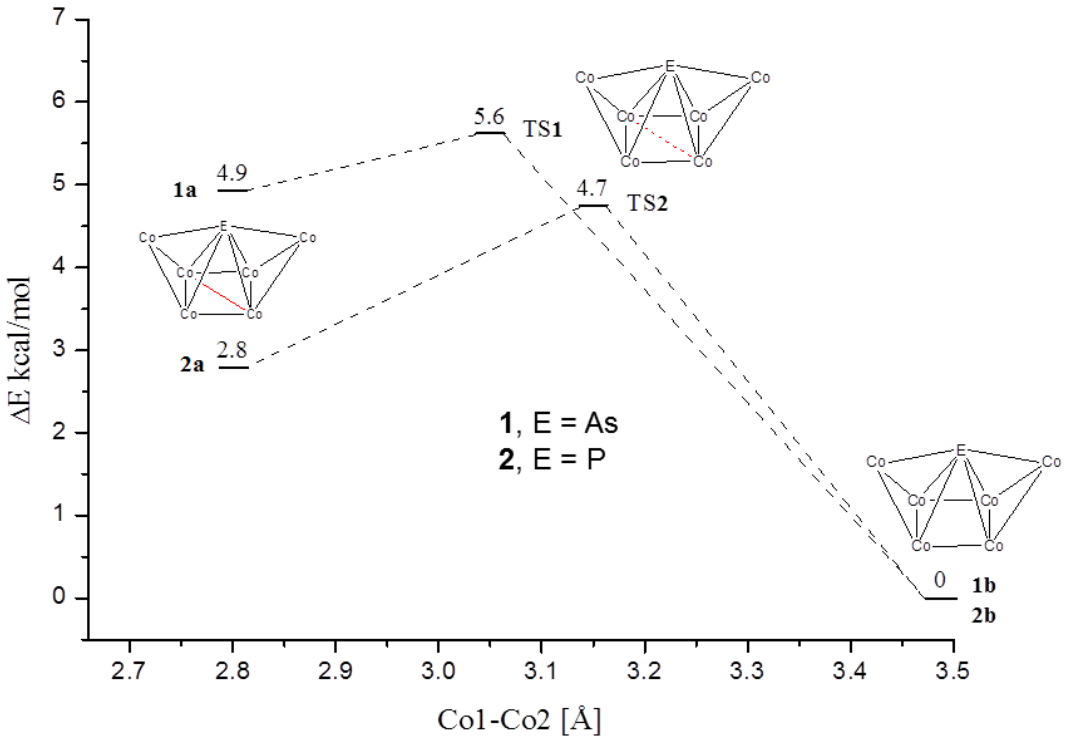

Periodical trends in $[Co_6E(CO)_{16}]^-$ clusters: structural, synthetic and energy changes produced by substitution of P with As.*

By

Roberto Della Pergola,[1,] Annalisa Sironi,[1] Valentina Colombo,[2] Luigi Garlaschelli,[2] Stefano Racioppi,[2] Angelo Sironi,[2,*] Piero Macchi.[3,*]*

1 Università di Milano-Bicocca- Dipartimento di Scienze Ambientali e della Terra, piazza della Scienza 1 – 20126 Milano Italy

2 Università degli Studi di Milano – Dipartimento di Chimica– Via Golgi, 19 – 20133 Milano Italy.

3 University of Bern - Department of Chemistry and Biochemistry, Freiestrasse 3 - 3012 Bern - Switzerland

roberto.dellapergola@unimib.it, angelo.sironi@unimi.it, piero.macchi@dcb.unibe.ch

ABSTRACT

The anionic cluster $[Co_6As(CO)_{16}]^-$ was synthesized through the reaction of $Na[Co(CO)_4]$ and arsenic acid in THF at room temperature. Crystallization from MeOH/2-propanol yielded two polymorphs that feature two slightly different isomers of the anion with the same PPh_4^+ cation. One of the isomers is very similar to the known $[Co_6P(CO)_{16}]^-$, formed by four edge fused triangles, partially wrapping the main group atom. The other isomer features a deformed cage, which differs mainly for a non-bonding Co-Co distance. The reasons for this unprecedented stereochemistry, and the factors which may trigger this isomer, have been investigated by DFT calculations.

Keywords: Cobalt, Arsenic, Metal cluster, Solid state structure, DFT calculations

*** Dedicated to Richard D. Adams for his outstanding contribution to Organometallic Chemistry**

1 Introduction

Thanks to their tendency to catenation, the heavier elements of group V (As, Sb, Bi) are particularly useful to construct molecular architectures, in combination with transition metals. The concern about this chemistry reached its highest point in the ’80-’90 years, and scientists focused essentially on structural aspects. Owing to this wide interest and this structural complexity, the field was synthetically illustrated by Greenwood [1] and was thoroughly reviewed by Whitmire.[2] Depending on the number of substituents (and the number of orbitals available for bonding), the main group element may act simply as an *exo*-skeleton ligand, be a well-defined vertex of the cluster skeleton, or occupy an interstitial position. Accordingly, AsR_3 are typical ligands in organometallic chemistry,[3] AsR fragments mimic $M(CO)_n$ moieties as vertices of the cage,[4] and As atoms may be fully surrounded by metals in clusters like $[Rh_{10}As(CO)_{22}]^{3-}$.[5] Transition and main group elements may play interchangeable roles, as shown by the complete series $As_{4-n}\{Co(CO)_3\}_n$ (n = 0,[6] 1,[7] 2,[8] 3 ,[9] 4[10]), which nicely illustrate the isolobal principle.[11]

Moreover, the construction of molecular architectures with different structural elements can be relevant for catalysis, since the formation of strong E-M bonds can confer extra stability to the molecules.[2] Accordingly, the quoted $[Rh_{10}As(CO)_{22}]^{3-}$ was self-assembled in conditions suitable for the homogeneous catalytic conversion of CO-H_2 mixtures into oxygenated compounds, and proved to be stable at partial pressures of CO as high as 260 atm.[5] More recently, this class of compounds has been used as single source for the preparation of binary and ternary phases which,[12] on turn, can find application for magnetic nanoparticles,[13] for the deposition of thin films [14] or for electrocatalysis.[15] In the latter field, the presence of the main group element helps in forming amorphous layers which are more catalytically active than bulk metal. In particular cobalt phosphides emerged as materials extremely active for both the hydrogen and oxygen evolution reactions (HER and OER).[16] For all these reasons, we devoted our attention to the synthesis of new Co-As clusters, trying to incorporate As atoms into small simple molecular

compounds, to be exploited as precursors of larger clusters, possibly with interstitial As atoms. The first result in this field is the isolation of the anion $[Co_6As(CO)_{16}]^-$, whose formula exactly matches that of the corresponding $[Co_6P(CO)_{16}]^-$ phosphide,[17] but differs from it for several structural and chemical aspects.

2 Results

2.1 Synthesis of $[Co_6As(CO)_{16}]^-$

As(I) and As(III) compounds such as $(AsPh)_6$ [4] or $(AsMe)_5$, [7] $AsCl_3$, [8] AsH_3 [9] or $AsPh_3$.[5] are typically used as sources of As. Conversely, we used PCl_5 as a source of P atoms in molecular cobalt clusters.[18] Since arsenic pentahalide are unstable and not commercially available, we tested the condensation of arsenic acid, (the hydrated $As_2O_5 \cdot 2H_2O$) with the sodium salt of $[Co(CO)_4]^-$. The reaction in THF at room temperature is smooth, as clearly evidenced by the darkening of the reaction mixture and the CO evolution. After about 1 day of stirring, the infrared spectrum of the reaction mixture shows the presence of new carbonyl compounds, together with some unreacted $[Co(CO)_4]^-$. When the As/Co molar ratio is lower than 1, the most intense bands are located at 2025, 2011 and 1808 cm^{-1}, assignable to the anion $[Co_6As(CO)_{16}]^-$; minor bands at higher wavenumbers denote the presence of neutral clusters, possibly the trimer $As_3Co_9(CO)_{24}$.[9] Conversely, if the As/Co molar ratio is increased to about 2, different uncharacterized species are formed, presumably richer in As and similar to the known $[Co_4Sb_2(CO)_{11}]^{2-}$ [19] and $[Co_4Bi_2(CO)_{11}]^{2-}$ anions.[20] Neutral and anionic species can be easily separated, by extracting the former with hydrocarbon solvents. After repeated washing with hexane, the salt $Na[Co_6As(CO)_{16}]$ is left behind. It can be dissolved in methanol, and layered with a dilute solution of PPh_4Cl in 2-propanol. Diffusion of the two solutions allows crystal growth. Alternatively, the compound can be isolated by precipitation with an ammonium or phosphonium salt, and used for further studies.

Among these, we are currently investigating the pyrolysis of $[Co_6As(CO)_{16}]^-$, in different solvents and at different temperatures.

2.2 Solid state structure

The samples obtained from methanol (method *3.2.1* in the experimental) contained crystals featuring two different morphologies (larger oblique prisms or smaller irregular chunks) both affording reasonable X-ray diffraction patterns (though, of different quality). Conventional single-crystal X-ray diffraction analysis afforded a full structural characterization of both species. They resulted to be two *conformational polymorphs* of the $[Co_6As(CO)_{16}][PPh_4]$ salt (hereinafter, α-**1**$[PPh_4]$ and β-**1**$[PPh_4]$). In fact, the two structures differ not only in the packing of the cationic and anionic moieties in the crystal (they feature, in fact, different space group types and lattice parameters) but also in the stereochemistry of the anionic cluster units (**1a** in α-**1**$[PPh_4]$ and **1b** in β-**1**$[PPh_4]$, respectively). Actually, **1a** and **1b** are constitutional isomers rather than conformers, given the presence or the absence of a weak Co-Co bond (*vide infra*). Thus, strictly speaking, the term 'conformational polymorphs' could be questionable here. However, we find this terminology substantially correct because **1a** and **1b** easily interconvert in solution (*vide infra*) and, more generally, metal carbonyl clusters often display ligands (and even metal-cage) fluxionalities in solution.[21]

α-**1**$[PPh_4]$, which crystallizes in the monoclinic space group $P2_1/c$, has a significantly higher density (1.812 *vs.* 1.758 g/cm^3) and a better crystallinity than β-**1**$[PPh_4]$, which crystallizes in the orthorhombic Pbca space group. As a matter of facts, eight small 'cavities' (each of ca. 10 Å^3) can be computed in β-**1**$[PPh_4]$. However, they are too small to host solvent molecules and, within the limits due to poor sample diffraction, do not contain any residual electron density. Thus, the

packing in β-**1**[PPh_4] appears to be truly less efficient than that in α-**1**[PPh_4] and must be correlated to the slightly different molecular geometries of **1a** and **1b**.

α-**1**[PPh_4] is isomorphous to the known [$Co_6P(CO)_{16}$][PPh_4] salt [17a]; accordingly, the stereochemistry of **1a** resembles that of [$Co_6P(CO)_{16}$]$^-$ (hereinafter, **2**) but for the differences inherent to the larger semi-interstitial atom (As *vs.* P). Thus, one may describe the anionic cluster cage as a folded chain of four edge-sharing triangles surrounding a "semi-interstitial" arsenic atom (see the folding angles Table 1). The anions are close to the idealized C_2 symmetry, with the two-fold axis passing through the heteroatom and the middle of the Co1-Co2 edge. However, the metal cage has an approximate C_{2v} symmetry. Accordingly, the Co-E bonds belong to two classes: the bonds to Co5 and Co6 atoms are significantly shorter than the other four. The Co-Co interactions can be divided into three classes: the four edges involving the external Co5 and Co6 atoms, the four shorter edges involving the central quadrilateral and the very long Col-Co2 edge, (see Table 1). All Co-Co bond distances are comparable to those found in many cobalt carbonyl clusters but the very long Col-Co2 interactions. Of the sixteen CO groups, fourteen are terminal and two symmetric edge-bridging. The cobalt atoms Co5 and Co6 bear three terminal carbonyls, whereas each of the other metal atoms is connected to one edge-bridging and to two terminal carbonyls.

The main difference between **1b** and **1a** concerns atoms Co1 and Co2 (see Figure 1 for a comparison between the two geometries). In fact, in **1b** the weak Co1-Co2 bond has an even longer distance, exceeding the limit to classify it as a bond. This elongation implies a rotation of ca. 20° about the pseudo three-fold axis of the $Co(CO)_3$ moieties of Co1 and Co2. Quite evident is especially the different orientation of the C15 and C16 carbonyls, bridging Co1-Co3 and Co2-Co4 bonds respectively (see Figure 1). This rearrangement preserves the overall C_2 symmetry of the anion but lowers (from C_{2v} to C_2) that of the cage.

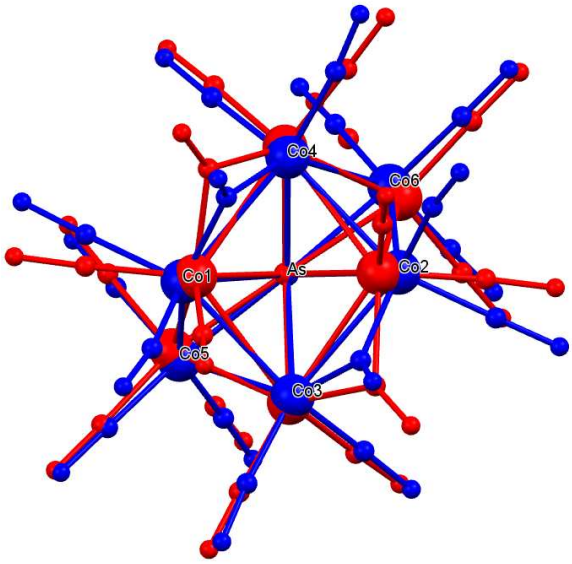

Figure 1: The overlay between structures **1a** (red) and **1b** (blue) as obtained from the corresponding **α-1** and **β-1** salts. Note in particular the longer Co1-Co2 contact in **1b** and the rotation of $Co(CO)_3$ moieties for Co1 and Co2. The root mean square deviation between the two geometries is 0.6 Å.

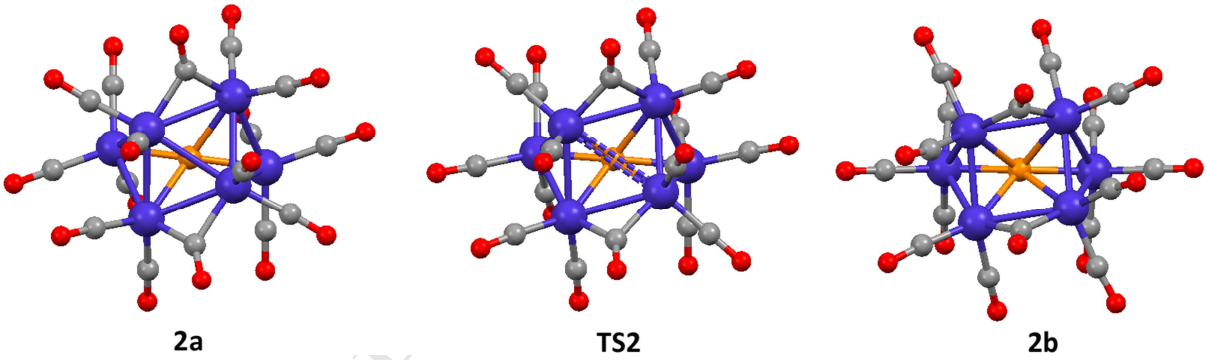

Figure 2: The isomer **2a**, **2b** and the transition state **TS2**, from M06/6-311+G(d,p) calculations.

Table 1. Selected bond distance and angles of isomers **1a**, **1b**, **2a**, **2b** and of the transition states **TS1** and **TS2** for $[Co_6X(CO)_{16}]^-$ (X = As, P) from X-ray diffraction or from theoretical calculations (M06/6-311+G(d,p)). The theoretical calculations are in C_2 symmetry.

	E = P				**E= As**				
	Expt.	**Theor.**			**Expt.**	**Theor.**			**Expt.**
	2a[17a]	**2a**	**TS2**	**2b**	**1a**	**1a**	**TS1**	**1b**	**1b**
		Selected Co-Co averaged distances							
Co1-Co2	2.935	2.801	3.150	3.487	2.944	2.800	3.045	3.489	3.457
Co5-Co(1,3), Co6-Co(2,4)	2.664 2.646	2.673 2.680	2.628 2.644	2.602 2.623	2.720 2.703	2.724 2.728	2.678 2.687	2.634 2.658	2.660 2,672
Co1-Co(3,4), Co2-Co(3,4)	2.574 2.575	2.670 2.570	2.660 2.555	2.631 2.538	2.607 2.595	2.695 2.564	2.682 2.564	2.671 2.544	2.636 2.579
Co5-Co6	4.105	4.153	4.107	4.092	4.385	4.441	4.436	4.408	4.364
		Selected E-Co (E = P, As) averaged distances							
E-Co(1,2,3,4)	2.263	2.255	2.274	2.287	2.371	2.378	2.392	2.400	2.390
E-Co(5,6)	2.170	2.193	2.181	2.181	2.265	2.283	2.281	2.279	2.266
	Dihedral angles (°) between edge sharing triangles								
Co(1,2,3)/Co(1,2,4)	143.4	135.4	145.3	159.9	145,0	137.5	144.2	159.3	159.7
Co(1,2,3)/Co(1,3,5)	122.9	123.8	120.1	115.4	125.1	126.0	124.3	118.9	119.1

Co(1,2,4)/Co(2,4,6)	122.0	123.8	120.1	115.4	124.3	126.0	124.3	118.9	118.4

Dihedral angles (°) between E, Co1,Co3 plane and carbonyls

E,Co(1,3),C(1)	105.7	112.3	112.4	88.9	105.0	111.1	109.6	87.7	85.2
E,Co(1,3),C(2)	-156.9	-148.7	-151.7	-176.1	-159.2	-152.2	-155.0	-176.5	-179.5
E,Co(1,3),C(15)	-64.8	-36.7	-63.1	-84.4	-69.8	-46.6	-64.4	-86.0	-86.7

2.3 Computational results

We have simulated the structures of anions **1a** and **1b**, as well as of the already known **2a** and of the not yet isolated **2b**. Moreover, we searched for energy pathways interconnecting the isomers and found the transition states **TS1** and **TS2**. All geometry optimizations and frequency calculations were performed using density functional theory (DFT) (see experimental section for more details). The calculated geometries of **1a**, **1b** and **2a** are in good qualitative and quantitative agreement with the experimental results (Table 1). Co1-Co2 distance is not very sensitive to the change of semi-interstitial atom, in fact **1a**/**2a** and **1b**/**2b** show similar lengths. Compared with X-ray data, the gas phase DFT calculations underestimate the Co1-Co2 distance in anions **a**, which further confirms the flexibility of this bond, very likely sensitive to the data collection conditions (such as P or T) when determined in the solid state. We tested also the possible role of the dielectric medium surrounding the anion and therefore optimized the geometries in various polarizable continuum model (PCM) [22], simulating solvents with different dielectric constant. However, this variable did not affect much the computed molecular geometries. The computed transition states show that the Co1-Co2 distance is in fact intermediate between **2a** and **2b** for the phosphide, whereas it results closer to **1a** for the arsenide. The bond distances and angles confirm that **TS1** is an early transition state (see Scheme 1). In Table 2, we report energy differences between isomers **a** and **b**. ΔE is the electronic energy difference which is independent from the medium (*in vacuo* or PCM returns the same value). From frequency calculations, we derived the corresponding enthalpies and Gibbs free energy differences (ΔH, ΔG), using thermal corrections at 1 atm and 298 K. ΔG_{PCM} represents the difference between free energy of solvation in THF obtained through PCM.

Table 2. The energy differences between isomers **a** and **b** for both **1** and **2**. Results are in kcal/mol

E	ΔE	ΔH	ΔG	ΔG_{PCM}
As	4.9	4.8	2.4	5.1
P	2.8	2.6	0.1	2.9

For both As and P derivatives, the isomers **b** are the most stable, however the thermodynamic driving force is certainly more pronounced for the As-derivative, whereas the Gibbs free energy difference (in pure gas phase) is negligible for the P-derivative.

We also analyzed the potential energy surface of these clusters. We carried out linear transit calculations *in vacuo*, by constraining various values of the Co1-Co2 distance, and computed the local transition states (TS) using the Synchronous Transit-Guided Quasi-Newton method [23]. Only **TS2** features a single imaginary frequency, corresponding to the stretching of Co1-Co2, whereas **TS1** shows an additional negative, albeit small, eigenvalue (-10.4 cm^{-1}), which corresponds to a real frequency in **TS2**. The discrepancy between anions **1** and **2** is probably due to the size of the integration grid, as for example observed by Ding and co-workers [24]. The overall reaction paths can be summarized as in scheme 1.

Scheme 1. Calculated energy [kcal/mol] pathway for isomerization.

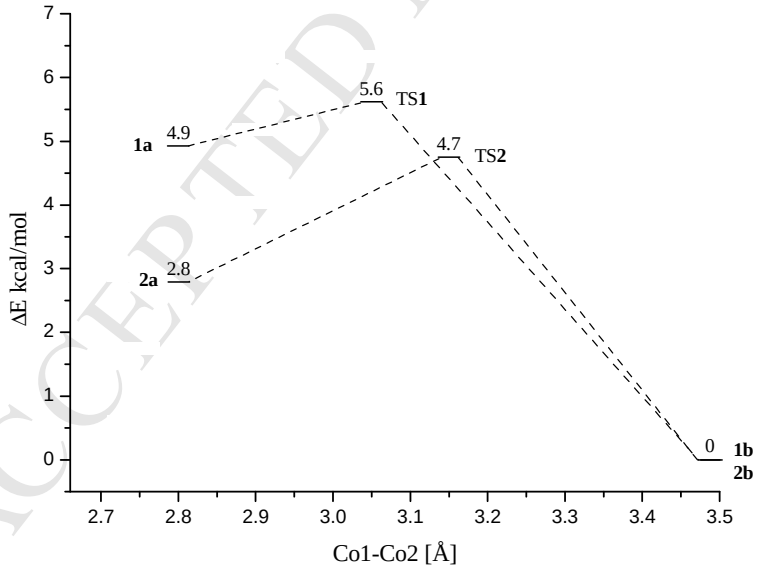

Here we note that the early transition state of **1** implies a much smaller barrier $\Delta E_{(TS\mathbf{1},\ \mathbf{1a})}$ compared with $\Delta E_{(TS\mathbf{2},\ \mathbf{2a})}$.

From these data, we conclude that: 1) in both cases, the isomer with the longest Co1-Co2 bond is the most stable, but the reaction equilibrium in the As derivative is certainly more shifted towards the "open" isomer **1b** (of course, this preference is fully consistent with the larger atomic radius of

As); 2) the kinetic barrier for this interconversion is higher for the P derivative, but anyway not very high and one should expect both species to be present in solution.

These conclusions should be merged with what previously observed on the crystal structure of the two isomers: isomers **a**, although less stable in isolation, are better stabilized by packing forces that counterbalance the unfavorable form of the cluster in polymorphs **α** . This may explain the reason why isomers **a** are always observed for both As and P, although being only the kinetic products. The calculated ΔE and ΔG may, in part, explain the reason why isomer **b** has not been isolated (yet) for the P derivative. In fact, the thermodynamic driving force toward **2b** is weaker than for **1b** and a higher kinetic barrier is present. Nevertheless, it is sensible to anticipate that an isomer of type **2b** should exist and could be in principle isolated.

3 Experimental

All the solvents were purified and dried by conventional methods and stored under nitrogen. All the reactions were carried out under oxygen-free nitrogen atmosphere using the Schlenk-tube technique.[25] Infrared spectra in solution were recorded on a Nicolet iS10 spectrophotometer, using calcium fluoride cells previously purged with N_2. A batch of $Na[Co(CO)_4]$ was prepared by dissolving 20 g of $Co_2(CO)_8$ in anhydrous THF (50 mL), and allowing it to react with small pieces of Na, until the IR bands of the reactant disappeared (2-3 days). The pale solution was filtered, and the THF was dried in vacuum, under moderate heating, to remove all traces of solvent.

ν(CO) in THF : 2010vw, 1887vs, 1857 m cm^{-1}

3.1 Synthesis of $Na[Co_6As(CO)_{16}]$

$Na[Co(CO)_4]$ (960 mg, 4.4 mmol) and $As_2O_5 \cdot xH_2O$ (480mg; 1.75 mmol) were suspended in THF (25 mL) and stirred at room temperature. A brown solution was formed, and some CO evolution was observed. After 1 day of stirring, the solution was filtered and the solvent was partially

removed in vacuum. 30 mL of heptane were added dropwise and the solution furtherly concentrated, until most of the product precipitated. The suspended solid was collected by filtration, washed with 10 mL of heptane, and dried.

ν(CO) in MeOH : 2075vw, 2027vs, 2014s, 1975w, 1809 m cm^{-1} (Figure 3)

3.2 Synthesis of $(PPh_4)[Co_6As(CO)_{16}]$

3.2.1 The crystals used for X-ray diffraction were obtained dissolving $Na[Co_6As(CO)_{16}]$, obtained as above, in the minimum amount of Methanol, and layering with a solution of PPh_4Cl in 2-propanol (ca. 0.5 mg/mL). After diffusion was completed, the mother liquors were eliminated by syringe. The solid residue was washed with 2-propanol and dried.

3.2.2 To obtain larger amounts of compound, $Na[Co_6As(CO)_{16}]$ was dissolved in Methanol and treated with a concentrated solution of PPh_4Cl in 2-propanol. After complete precipitation occurred, the solid was collected by filtration, washed with 2-propanol and dried.

Typical yields 45-50% (calculated on Co).

Calc for $C_{40}H_{20}AsCo_6O_{16}P$ C 39.51 ; H 1.66 %; found C 39.7 ; H 1.4 %.

ν(CO) in THF : 2074vw, 2027vs, 2012s, 1975w, 1954w, 1809 m cm^{-1} (figure 3)

3.3 X-ray Single Crystal Structure Determinations.

3.3.1 Intensity measurements. An oblique prismatic crystal of compound (α-**1**[PPh_4]) of dimensions 0.33 × 0.18 × 0.17 mm and a irregular-shaped crystal of compound *(*β-**1**[PPh_4]*)* of dimensions 0.13 × 0.12 × 0.12 mm, both mounted on glass fibers in the air, were transferred to an Enraf-Nonius CAD4 automated diffractometer. Graphite-monochromated Mo-Kα, radiation was used. In both cases the setting angles of 25 random reflections ($16 < 2\theta < 22°$) were used to determine by least-squares fit accurate cell constants and orientation matrices. The two data collections were performed by the ω-scan method, within the limits $3 < 2\theta < 25°$, using a variable scan speed (from

3 to 20° min^{-1}) and a variable scan range of *(α*+0.35tanθ)" [*α*= 1.0°(α-**1**[PPh_4]) and 1.2°(β-**1**[PPh_4])], with a 25% extension at each end for background determination. Reflections corresponding to the *±h, +k, +l* and *+h, +k, +l* indices were collected for compounds (α-**1**[PPh_4]) and (β-**1**[PPh_4]), respectively. The total numbers of reflections measured were 7788 (α-**1**[PPh_4]) and 7946 (β-**1**[PPh_4]). Three standard reflections were measured every 3 h and no significant crystal decay was observed in both data collections. The intensities were corrected for Lorentz and polarization effects. An empirical absorption correction was applied in both cases based on ψ scans [26] (ψ 0-360° every 10°) of suitable reflections with χ values close to 90°; the maximum, minimum, and average relative transmission values were 1.00, 0.55, and 0.84 for complex (α-**1**[PPh_4]) and 1.00, 0.72, and 0.85 for (β-**1**[PPh_4]), respectively. Two sets of 3 897 (α-**1**[PPh_4]) and 2 168 *(*β-**1**[PPh_4]*)* independent significant reflections, with *I* >3 σ(I), were used in the structure solutions and refinements.

3.3.2 Structure solutions and refinements. Both structures were solved by direct methods (SHELXS)

The refinements were carried out by full-matrix least-squares methods using SHELXL-2014/7.[27] Anisotropic thermal parameters were assigned only to phosphorous and the anionic atoms.

Phenyls have been treated as rigid bodies with hydrogen atoms riding on their carbon atoms on idealized positions.

Final Fourier difference maps showed residual peaks not exceeding *ca.* 0.8 e/ A^{-3}. The final values of the conventional agreement indices R_1 and wR_2 [$I > 2\sigma(I)$] were 0.0414 and 0.0828 for compound α-**1**[PPh_4] and 0.0483 and 0.0923 for compound β-**1**[PPh_4]**,** respectively.

The final positional parameters are listed in Tables **4** and **5** for α-**1**[PPh_4] and β-**1**[PPh_4]**,** respectively.

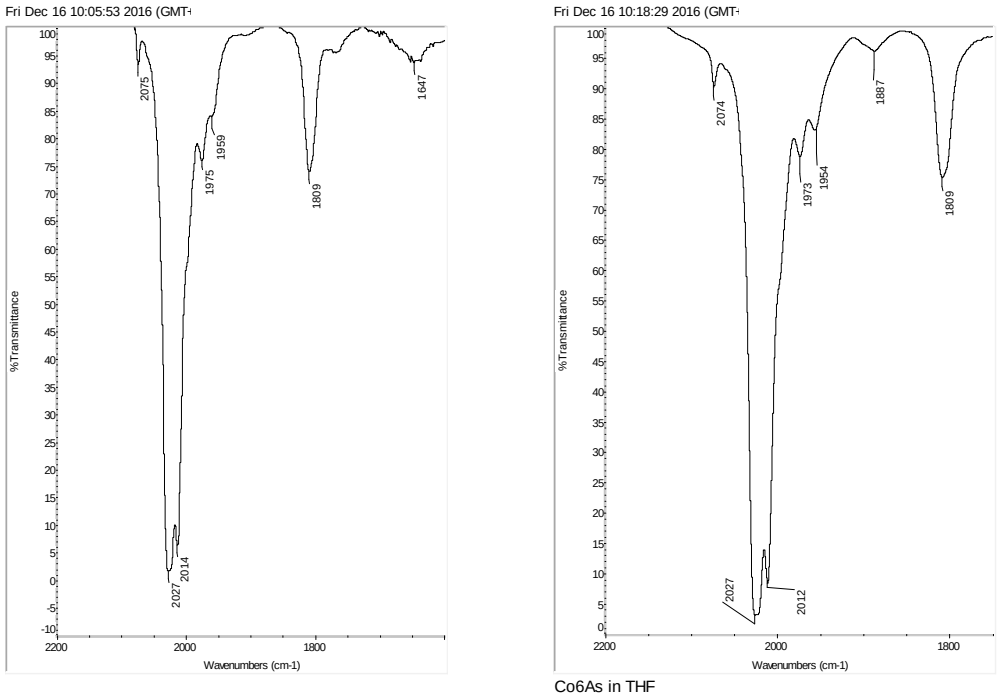

Figure 3 – The IR spectra of $Na[Co_6As(CO)_{16}]$ in MeOH (left) and $PPh_4[Co_6As(CO)_{16}]$ in THF (right)

3.4. Computational details

All the calculations were performed with GAUSSIAN 09 package [28]. Initial structures of **1a**, **1b** and **2a** were taken from single crystal X-ray diffraction results. Full geometry optimizations of the isomers were carried out considering C_2 point group, followed by frequency calculation to confirm the nature of the minima and to obtain thermochemical data. The functional M06[29] was chosen with 6-311+G(d,p) basis for all the atoms. The same level of theory (M06/6-311+G(d,p)) was used for both geometry optimizations and frequencies calculations. Solvent effect was accounted for subsequent geometry optimizations using the Polarizable Continuum Model (PCM) [22]. A standard cavity was used, and the dielectric constant of tetrahydrofuran (THF) was 7.4257, and the initial structures were taken from the optimizations in gas phase. Cartesian coordinates corresponding to all structures are given in the *Supporting Information*.

4 Conclusions

The reaction between $Na[Co(CO)_4]$ and arsenic acid yields $[Co_6As(CO)_{16}]^-$, which is the first known anionic Co-As derivative, and other uncharacterized species. $[Co_6As(CO)_{16}]^-$ and $[Co_6P(CO)_{16}]^-$ share a quite similar geometry, however we observed for the As derivative an additional isomer (featuring one absent Co-Co bond), not yet known for the P-substituted species. Theoretical calculations predict for both species that the larger cage is the more stable isomer, although the experimentally observed packing for this species is much less efficient, which may explain its more elusive behaviour.

The conversion of $[Co_6As(CO)_{16}]^-$ into larger clusters, possibly with interstitial As atoms will be explored, as a step toward new Co-As materials. Moreover, we plan to carry out thorough characterizations of the electron density distributions in both isomers.

Acknowledgements

This work was supported by University of Milano Bicocca (RDP, AS).

PM and SR thank the Swiss National Science Foundation (project 160157) for financial support.

Table 3 Crystal data and experimental details for α-**1**[PPh_4] and β-**1**[PPh_4].

Identification code	α-1[PPh_4]	β-1[PPh_4]
Empirical formula	C_{40} H_{20} As Co_6 O_{16} P	C_{40} H_{20} As Co_6 O_{16} P
Formula weight	1216.03	1216.03
Temperature	298(2) K	298(2) K
Wavelength	0.71073 A	0.71073 A
Crystal system	Monoclinic	Orthorhombic
Space group	P 2_1/c	P b c a
a/Å	10.082(3)	21.191(5)
b/Å	21.266(5)	20.370(5)
c/Å	20.791(5)	21.284(5)
α/°	90.0	90.0
β/°	91.05(2)	90.0
γ/°	90.0	90.0
V/Å^3	4457(3)	9187(4)
Z, Calculated density /Mg m^{-3}	4, 1.812	8, 1.758
Absorption coefficient /mm^{-1}	3.023	2.933
F(000)	2392	4784
Crystal size /mm	0.33 × 0.18 × 0.17	0.13 × 0.12 × 0.12
θ-range/°	2.998 to 24.974	3.189 to 24.898
Limiting indices	-11≤ h ≤11, 0≤ k ≤25, 0≤ l ≤24	0≤ h ≤25, 0≤ k ≤24, 0≤ l ≤25
Reflections collected/unique	7788 / 7788	7946 / 7946
Completeness to *θ*-max	99.8 %	99.4 %
Absorption correction	Psi-scan	
Max. and min. transmission	1.0 and 0.78	1.00 and 0.91
Refinement method	Full-matrix least-squares on F^2	
Data / restraints / parameters	7788 / 0 / 409	7946 / 0 / 409
Goodness-of-fit (F^2)	0.995	0.902
R_1, wR_2 [$I > 2\sigma(I)$]	0.0414, 0.0828	0.0483, 0.0923
R_1, wR_2 (all data)	0.1476, 0.1010	0.2961, 0.1329
Largest diff. peak and hole/e Å^{-3}	0.705, -0.504	0.804, -1.024

†Electronic Supplementary Information (ESI) available: CCDC…… (**1a**) and CCDC …… (**1b**) contains the supplementary crystallographic data for compounds α-**1**[PPh_4] and β-**1**[PPh_4]. These data can be obtained free of charge from The Cambridge Crystallographic Data Centre via www.ccdc.cam.ac.uk/data_request/cif.

Table 4. Atomic coordinates (x 10^4) and equivalent isotropic displacement parameters (A^2x 10^3) for α-1[PPh_4]. U(eq) is defined as one third of the trace of the orthogonalized Uij tensor.

Co(1)	9810(1)	2567(1)	9671(1)	46(1)
Co(2)	10899(1)	3140(1)	10857(1)	50(1)
Co(3)	9387(1)	3727(1)	10020(1)	50(1)
Co(4)	10162(1)	1980(1)	10760(1)	45(1)
Co(5)	7269(1)	2985(1)	9770(1)	47(1)
Co(6)	9064(1)	2698(1)	11684(1)	54(1)
C(1)	9075(7)	2142(3)	9031(3)	64(2)
O(1)	8655(6)	1841(3)	8615(3)	103(2)
C(2)	11006(8)	2998(3)	9257(3)	73(2)
O(2)	11865(6)	3214(3)	8975(3)	105(2)
C(3)	12497(8)	2832(3)	10717(4)	70(2)
O(3)	13549(5)	2661(3)	10624(3)	99(2)
C(4)	11168(7)	3532(4)	11584(4)	74(2)
O(4)	11470(5)	3819(3)	12021(3)	115(2)
C(5)	9493(8)	4169(3)	9288(4)	75(2)
O(5)	9561(7)	4467(3)	8836(3)	126(3)
C(6)	8578(7)	4288(3)	10515(4)	71(2)
O(6)	8071(6)	4630(3)	10847(3)	113(2)
C(7)	11493(7)	1659(3)	11235(3)	62(2)
O(7)	12305(5)	1435(3)	11545(3)	91(2)
C(8)	9039(7)	1332(3)	10682(3)	62(2)
O(8)	8335(6)	924(3)	10612(3)	100(2)
C(9)	7322(7)	3262(3)	8951(4)	60(2)
O(9)	7315(6)	3418(3)	8430(2)	92(2)
C(10)	6403(7)	2250(3)	9746(3)	60(2)
O(10)	5848(6)	1790(3)	9741(3)	108(2)
C(11)	6103(7)	3498(3)	10140(3)	61(2)
O(11)	5382(5)	3822(3)	10385(3)	92(2)
C(12)	10254(8)	2414(4)	12264(3)	83(2)
O(12)	10970(6)	2238(4)	12653(3)	137(3)
C(13)	7793(8)	2117(4)	11783(3)	65(2)
O(13)	6974(6)	1755(3)	11839(3)	94(2)
C(14)	8363(6)	3399(4)	12035(3)	64(2)
O(14)	7929(6)	3831(3)	12263(3)	95(2)
C(15)	10921(7)	1881(3)	9930(3)	58(2)
O(15)	11711(5)	1559(3)	9692(2)	90(2)
C(16)	11115(7)	3898(3)	10368(3)	59(2)
O(16)	11921(5)	4287(2)	10318(3)	92(2)
As	8678(1)	2837(1)	10614(1)	38(1)
P	5812(2)	-383(1)	12095(1)	42(1)
C(111)	5652(4)	-1219(2)	12185(2)	47(2)
C(112)	5862(4)	-1605(2)	11657(2)	66(2)
C(113)	5775(5)	-2254(2)	11721(2)	84(2)
C(114)	5477(5)	-2518(2)	12312(2)	88(2)
C(115)	5266(4)	-2132(2)	12841(2)	83(2)
C(116)	5353(4)	-1483(2)	12777(2)	63(2)

C(121)	7509(3)	-170(2)	11986(2)	41(1)
C(122)	8059(4)	342(2)	12310(2)	56(2)
C(123)	9390(4)	491(2)	12234(2)	73(2)
C(124)	10171(3)	127(2)	11834(2)	75(2)
C(125)	9621(4)	-384(2)	11510(2)	88(2)
C(126)	8290(4)	-533(2)	11586(2)	67(2)
C(131)	4832(3)	-149(2)	11410(2)	46(2)
C(132)	5152(3)	396(2)	11079(2)	62(2)
C(133)	4345(4)	601(2)	10571(2)	78(2)
C(134)	3219(4)	261(2)	10396(2)	69(2)
C(135)	2899(3)	-285(2)	10728(2)	63(2)
C(136)	3706(4)	-489(2)	11235(2)	55(2)
C(141)	5227(4)	13(2)	12792(2)	45(2)
C(142)	5874(3)	-55(2)	13383(2)	53(2)
C(143)	5388(4)	247(2)	13923(2)	64(2)
C(144)	4255(4)	617(2)	13871(2)	74(2)
C(145)	3607(3)	685(2)	13280(2)	78(2)
C(146)	4093(4)	383(2)	12740(2)	63(2)

Table 5. Atomic coordinates (x 10^4) and equivalent isotropic displacement parameters (A^2 x 10^3) for β-1[PPh_4]. U(eq) is defined as one third of the trace of the orthogonalized Uij tensor.

Atom	x	y	z	U(eq)
Co(1)	-915(1)	617(1)	2579(1)	45(1)
Co(2)	16(1)	-776(1)	2543(1)	48(1)
Co(3)	-262(1)	105(1)	1679(1)	45(1)
Co(4)	-370(1)	-75(1)	3474(1)	45(1)
Co(5)	9(1)	1318(1)	2079(1)	51(1)
Co(6)	869(1)	-179(1)	3270(1)	56(1)
As	209(1)	392(1)	2639(1)	42(1)
C(1)	-1542(5)	535(5)	2044(5)	66(3)
O(1)	-1990(4)	511(5)	1745(4)	116(3)
C(2)	-1187(4)	1318(5)	3007(5)	55(3)
O(2)	-1383(4)	1756(4)	3275(4)	84(3)
C(3)	-371(5)	-1398(5)	2965(5)	58(3)
O(3)	-629(4)	-1847(4)	3185(4)	100(3)
C(4)	603(5)	-1274(5)	2157(5)	56(3)
O(4)	983(4)	-1588(4)	1927(4)	111(3)
C(5)	441(5)	-70(5)	1250(5)	61(3)
O(5)	900(4)	-170(4)	979(4)	91(3)
C(6)	-764(5)	253(5)	1020(5)	58(3)
O(6)	-1045(4)	338(4)	582(3)	85(3)
C(7)	-528(5)	-682(6)	4072(5)	64(3)
O(7)	-641(4)	-1028(4)	4464(4)	103(3)
C(8)	-349(5)	614(6)	3999(5)	72(3)
O(8)	-339(5)	1043(4)	4334(4)	116(3)
C(9)	81(5)	1920(5)	2685(5)	56(3)
O(9)	117(4)	2305(4)	3079(4)	87(3)
C(10)	-601(5)	1623(5)	1572(5)	62(3)
O(10)	-976(4)	1830(4)	1241(4)	97(3)
C(11)	714(5)	1405(5)	1650(5)	62(3)
O(11)	1172(4)	1487(4)	1366(4)	96(3)
C(12)	1534(5)	-279(6)	2783(6)	90(4)
O(12)	1966(4)	-357(6)	2466(5)	157(5)
C(13)	841(5)	-912(6)	3733(6)	78(4)
O(13)	864(4)	-1375(4)	4037(5)	118(3)
C(14)	1109(5)	452(6)	3807(6)	76(4)
O(14)	1271(4)	862(4)	4126(4)	112(3)
C(15)	-1209(4)	-38(5)	3154(4)	48(3)
O(15)	-1698(3)	-294(3)	3253(3)	69(2)
C(16)	-572(5)	-772(5)	1868(5)	55(3)
O(16)	-965(3)	-1121(3)	1657(3)	76(2)
P	1942(1)	2865(1)	4616(1)	45(1)
C(111)	2202(3)	2212(3)	5108(3)	50(3)
C(112)	2703(3)	1815(3)	4925(2)	63(3)
C(113)	2942(2)	1347(3)	5337(3)	72(3)

C(114)	2680(3)	1276(3)	5932(3)	62(3)
C(115)	2179(3)	1673(3)	6115(2)	68(3)
C(116)	1940(2)	2141(3)	5703(3)	60(3)
C(121)	2351(3)	3605(3)	4808(3)	46(3)
C(122)	2323(3)	4134(3)	4396(2)	61(3)
C(123)	2603(3)	4728(3)	4557(3)	73(3)
C(124)	2911(3)	4793(3)	5130(3)	86(4)
C(125)	2939(3)	4264(4)	5542(3)	95(4)
C(126)	2659(3)	3671(3)	5381(3)	77(4)
C(131)	2100(3)	2677(3)	3817(3)	46(3)
C(132)	2695(3)	2801(3)	3570(3)	82(4)
C(133)	2832(3)	2627(4)	2954(4)	98(4)
C(134)	2374(4)	2328(4)	2584(3)	105(4)
C(135)	1778(4)	2204(4)	2831(4)	133(6)
C(136)	1641(3)	2378(4)	3448(4)	98(4)
C(141)	1114(2)	2984(3)	4750(3)	48(3)
C(142)	874(3)	3615(3)	4814(3)	50(3)
C(143)	228(3)	3711(3)	4881(3)	70(3)
C(144)	-178(2)	3174(3)	4884(3)	72(3)
C(145)	63(3)	2543(3)	4820(3)	84(4)
C(146)	709(3)	2448(2)	4753(3)	67(3)

REFERENCES

[1]N.N.Greenwood, A.Earnshaw, *Chemistry of the Elements*, (2nd ed.) - Butterworth-Heinemann, Oxford, 1997 pp 583

[2] K.H.Whitmire, Adv. Organometallic Chem. 42 (1998) 1-145

[3] P. Macchi, D.M.Proserpio, A.Sironi, J. Am. Chem. Soc., 120 (1998) 13429–13435

[4] a) R.M.De Silva, M.J.Mays, J.E.Davies, P.R.Raithby, M.A.Rennie, G.P.Shields, J.Chem.Soc.,Dalton Trans., (1998) 439 b) A.L.Rheingold, P.J.Sullivan, J.Chem.Soc.,Chem Commun., (1983) 39

[5] J.L.Vidal, Inorg. Chem. 20 (1981) 243-249

[6] N.N.Greenwood, A.Earnshaw, *Chemistry of the Elements*, (2nd ed.) - Butterworth-Heinemann, Oxford, 1997 pp 551

[7] A.S.Foust, M.S.Foster, L.F.Dahl, J. Am. Chem. Soc., 91 (1969) 5631–5633

[8]A.S.Foust, M.S.Foster, L.F.Dahl, J. Am. Chem. Soc., 91 (1969) 5633–5635

[9] L.J.Arnold, K.M.Mackay, B.K.Nicholson, J.Organomet.chem., 387 (1990) 197

[10] a) C.H. Wei Inorg. Chem., 8 (1969) 2384–2397 b) L.J.Farrugia, D.Braga, F.Grepioni, J.Organomet.Chem., 573 (1999) 60-66

[11] R.Hoffmann, Angew. Chem. Int. Ed. 21 (1982) 711–724

[12] D.E.Schipper, B.E.Young, K.H.Whitmire, Organometallics 35 (2016) 471−483

[13] F.-R. Klingan, A. Miehr, R.A. Fischer, W.A. Herrmann Appl. Phys. Lett. 67 (1995) 822-824

[14] P.Desai,N.Ashokaan, J.Masud,A.Pariti, M.Nath, Mater. Res. Express 2 (2015) 036102

[15]a) A. Rabis, P.Rodriguez, T.J.Schmidt, ACS Catal, 2 (2012) 864-890 b) N.A.Vante, W.Jaegermann, H.Tributsch, W.Honle, K.Yvon, J. Am. Chem. Soc., 109 (1987) 3251-3257

[16] a) J.Wang, W.Cui, Q.Liu, Z. Xing, A.M.Asiri, X.Sun Adv. Mater. 28 (2016) 215–230 b) P.Wang, F.Song, R.Amal, Y.H. Ng, X.Hu, ChemSusChem 9 (2016) 472 –477 c) N. Jiang,B.You, M. Sheng, Y. Sun, Angew.Chem. Int.Ed. 54 (2015) 6251 –6254 d) E. J. Popczun, C. G. Read, R. E. Schaak Angew. Chem. Int. Ed. 53 (2014) 5427 –5430

[17] a) P.Chini, G.Ciani, S.Martinengo, A.Sironi, J.Chem.Soc., Chem.Commun, (1979) 188; b) G.Ciani, A.Sironi, J.Organomet.Chem., 241 (1983) 385-393

[18] G.Ciani, A.Sironi, S.Martinengo, L.Garlaschelli, R.della Pergola, P.Zanello, F.Laschi, N.Masciocchi, Inorg.Chem., 40 (2001) 3905-3911

[19] T.A.Albright, K.A.Yee, J.-Y.Saillard, S.Kahal, J.-F.Halet, J.S.Leigh, K.H.Whitmire, Inorg.Chem., 30, (1991) 1179-1190,

[20] S.Martinengo, G.Ciani, J.Chem.Soc., Chem.Commun., (1987) 1589

[21] B.T.Heaton, L.Strona, R. Della Pergola, J.L.Vidal, R.c.Schoening, J.Chem.Soc., Dalton Trans., (1983) 1941-1947

[22] Tomasi, J.; Mennucci, B.; Cammi, R. Chem. Rev., 105 **(**2005) 2999–3093.

[23] C.Peng, P. Y.Ayala, H. B.Schlegel, M.J.J. Frisch, Comp. Chem., 17 (1996) 49-56.

[24] H.Ding, Y.Lu, Y.Xie, H.Liu, H.F.Schaefer, J. Chem. Theory Comput., 11 (2015) 940-949.

[25] D.F.Shriver, M.A.Drezdzon, *The Manipulation of air-sensitive compounds*, 2nd ed. (1986) Wiley New York.

[26] A.C.T. North, D.C. Phillips, F.S. Mathews, Acta Crystallogr., Sect. A: Found. Crystallogr., 24 (1968) 351-359

[27] G.M. Sheldrick, Acta Cryst. C71 (2015). 3-8

[28] Gaussian 09, Revision D.01,M. J. Frisch, G. W. Trucks, H. B. Schlegel, G. E. Scuseria, M. A. Robb, J. R. Cheeseman, G. Scalmani, V. Barone, B. Mennucci, G. A. Petersson, H. Nakatsuji, M. Caricato, X. Li, H. P. Hratchian, A. F. Izmaylov, J. Bloino, G. Zheng, J. L. Sonnenberg, M. Hada, M. Ehara, K. Toyota, R. Fukuda, J. Hasegawa, M. Ishida, T. Nakajima, Y. Honda, O. Kitao, H. Nakai, T. Vreven, J. A. Montgomery, Jr., J. E. Peralta, F. Ogliaro, M. Bearpark, J. J. Heyd, E. Brothers, K. N. Kudin, V. N. Staroverov, T. Keith, R. Kobayashi, J. Normand, K. Raghavachari, A. Rendell, J. C. Burant, S. S. Iyengar, J. Tomasi, M. Cossi, N. Rega, J. M. Millam, M. Klene, J. E. Knox, J. B. Cross, V. Bakken, C. Adamo, J. Jaramillo, R. Gomperts, R. E. Stratmann, O. Yazyev, A. J. Austin, R. Cammi, C. Pomelli, J. W. Ochterski, R. L. Martin, K. Morokuma, V. G. Zakrzewski, G. A. Voth, P. Salvador, J. J. Dannenberg, S. Dapprich, A. D. Daniels, O. Farkas, J. B. Foresman, J. V. Ortiz, J. Cioslowski, and D. J. Fox, Gaussian, Inc., Wallingford CT, (2013).

[29] Y.Zhao, G.D.Truhlar, Theor. Chem. Account, 120 **(**2008) 215–241.

Highlights

- The synthesis of a new Co-As cluster, namely $[Co_6As(CO)_{16}]^-$, is reported.
- The cluster has composition and structure similar to the corresponding phosphide
- Two isomers of the clusters were isolated in the solid state, differing for the number of Co-Co bond
- DFT studies have shown that the isomer with less Co-Co bond is the more stable, both for P and As
- The energy difference for the two isomers is more pronounced for As, in keeping with the larger atomic dimensions
- The less stable isomer is stabilized by more efficient crystal packing